LETTERS

Modelling West Antarctic ice sheet growth and collapse through the past five million years

David Pollard[1] & Robert M. DeConto[2]

The West Antarctic ice sheet (WAIS), with ice volume equivalent to ~5 m of sea level[1], has long been considered capable of past and future catastrophic collapse[2–4]. Today, the ice sheet is fringed by vulnerable floating ice shelves that buttress the fast flow of inland ice streams. Grounding lines are several hundred metres below sea level and the bed deepens upstream, raising the prospect of runaway retreat[3,5]. Projections of future WAIS behaviour have been hampered by limited understanding of past variations and their underlying forcing mechanisms[6,7]. Its variation since the Last Glacial Maximum is best known, with grounding lines advancing to the continental-shelf edges around ~15 kyr ago before retreating to near-modern locations by ~3 kyr ago[8]. Prior collapses during the warmth of the early Pliocene epoch[9] and some Pleistocene interglacials have been suggested indirectly from records of sea level and deep-sea-core isotopes, and by the discovery of open-ocean diatoms in subglacial sediments[10]. Until now[11], however, little direct evidence of such behaviour has been available. Here we use a combined ice sheet/ice shelf model[12] capable of high-resolution nesting with a new treatment of grounding-line dynamics and ice-shelf buttressing[5] to simulate Antarctic ice sheet variations over the past five million years. Modelled WAIS variations range from full glacial extents with grounding lines near the continental shelf break, intermediate states similar to modern, and brief but dramatic retreats, leaving only small, isolated ice caps on West Antarctic islands. Transitions between glacial, intermediate and collapsed states are relatively rapid, taking one to several thousand years. Our simulation is in good agreement with a new sediment record (ANDRILL AND-1B) recovered from the western Ross Sea[11], indicating a long-term trend from more frequently collapsed to more glaciated states, dominant 40-kyr cyclicity in the Pliocene, and major retreats at marine isotope stage 31 (~1.07 Myr ago) and other super-interglacials.

Large-scale modelling of the WAIS requires an ice-sheet model that combines the flow regimes of grounded and floating ice efficiently enough to allow simulations of $\sim 10^5$ yr or more. This is challenging, because the scaled equations for the two regimes are very different, and near the grounding line they interact in a boundary-layer zone that affects the large-scale dynamics[5]. More rigorous higher-order flow models without separate scalings are currently too computationally expensive for long-term continental applications[13]. Our approach simply combines the scaled sheet and shelf equations[12], while capturing grounding-line effects by imposing a new mass-flux condition[5]. Other standard model components predict variations in ice thickness, ice temperatures, and bedrock elevation below the ice (see Methods).

The multi-million-year timescales considered here are beyond the capability of most climate models to provide the necessary time-continuous forcings required by the ice sheet model. Instead we use techniques similar to those used in previous studies[6,7] and drive the model with simple parameterizations of surface mass balance, air temperature and specified sea level. A new parameterization of sub-ice-shelf ocean melt based on modern observations[14–16] accounts for changes in the shape of coastlines and distance from the ice edge to open ocean[17] (see Methods).

Before considering long-term simulations, it is helpful to examine the link between equilibrated ice-sheet states and the strength of various forcing mechanisms (Fig. 1) representative of extreme interglacial (left of graphs), modern interglacial (middle) and full glacial (right) conditions. In between the values shown, each forcing is linearly interpolated along the x axis. This closely approximates how they co-vary in long-term simulations, but not exactly due to independent influences of $\delta^{18}O$ and austral insolation (see below). The envelopes of ocean-melt values are chosen so that complete WAIS collapse and full glacial expansion are just attained.

Figure 1a indicates a smoothly varying response from intermediate to large WAIS sizes, with sharper transitions into and out of extreme interglacials (collapses), and also back from full glacial to intermediate states. This behaviour is seen in long-term simulations and animations (Supplementary Videos 1, 2), with rapid transitions taking from one to several thousand years. The whole range of Antarctic states in the model is more or less 'one-dimensional', that is, the Ross, Weddell and Amundsen Sea sectors of the WAIS usually retreat and expand in unison, resulting in just one type of configuration for a given total ice volume. This suggests that the broad-scale Plio-Pleistocene history of the WAIS is represented at the ANDRILL AND-1B drill site[11], and persistent absence of a Ross ice shelf is indeed indicative of major WAIS retreat.

The relative importance of individual forcing mechanisms is shown in Fig. 1b. For modern to extreme interglacial conditions, changes in surface climate and sea level are relatively small, while changes in ocean melt are dominant via their effect on ice-shelf buttressing. For modern to glacial conditions, a combination of ocean-melt and sea-level changes is needed to produce realistic WAIS expansion[6,7]. Changes in precipitation and surface temperature have significant, but largely cancelling, effects: without reduced precipitation in cooler climates, glacial volumes are too large ('no ΔP', Fig. 1b); without the effects of cooler surface temperatures on internal ice temperatures, viscosities and basal sliding, glacial ice flows too easily and volumes are too small ('no ΔT', Fig. 1b).

A five-million-year simulation (Fig. 2) is performed from the early Pliocene to present, with the long-term variation of each forcing mechanism parameterized largely as a function of deep-sea-core $\delta^{18}O$ (ref. 18). Sea level over most of this interval is dominated by Northern Hemispheric ice volume, and can be readily prescribed in proportion to $\delta^{18}O$. The responses of Antarctic surface temperature and precipitation to Pleistocene glacial cycles are also reasonably constrained by climate studies and observations, and we adapt established

[1]Earth and Environmental Systems Institute, Pennsylvania State University, University Park, Pennsylvania 16802, USA. [2]Department of Geosciences, University of Massachusetts, Amherst, Massachusetts 01003, USA.

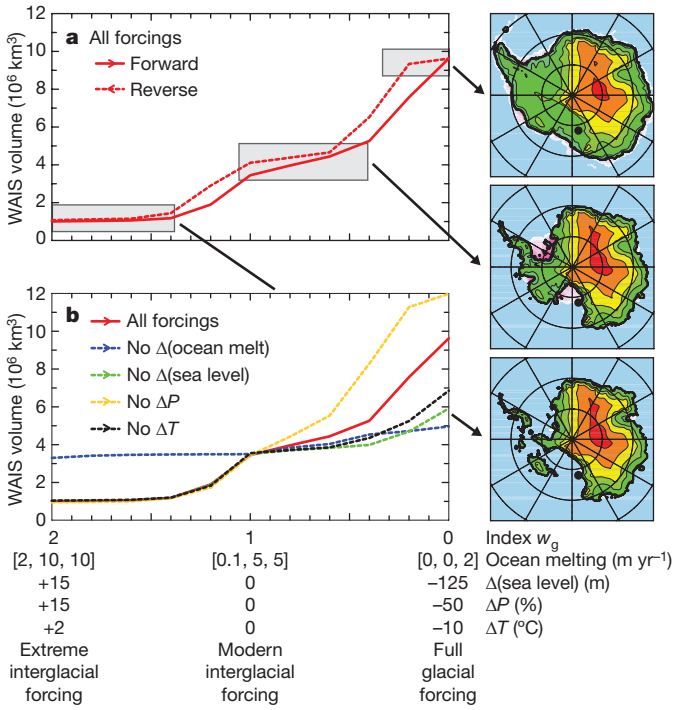

Figure 1 | Equilibrium West Antarctic ice volumes versus specified forcing, and ice-sheet configurations. Left panels, ice volumes. The four forcing mechanisms are sub-ice-shelf oceanic melting and departures of sea level, annual precipitation ΔP and temperature ΔT from present. The three sets of forcing values represent climates for extreme interglacial (left), modern interglacial (middle), and full glacial (right). In between, each forcing is linearly interpolated along the x-axis (w_g, see equation (6) in Methods). The triplets of sub-ice oceanic melt rates are for protected, exposed-shelf, and deep-ocean regions—[M_p, M_e, M_d], equations (7) and (8) in Methods. **a**, All forcing mechanisms changed together. Solid (dashed) curves are generated with ice sheets initialized from prior solutions representing cooling (warming) trends. The slight difference between the two curves contrasts with the much larger hysteresis of East Antarctica, where surface melt and not sub-ice-shelf melt is the dominant ablation process[32]. **b**, With one mechanism held constant at its modern value, and all others changed. Right panels, ice sheet configurations representative of the three climatic states, with the black dot showing the location of the ANDRILL AND-1B drill site[11].

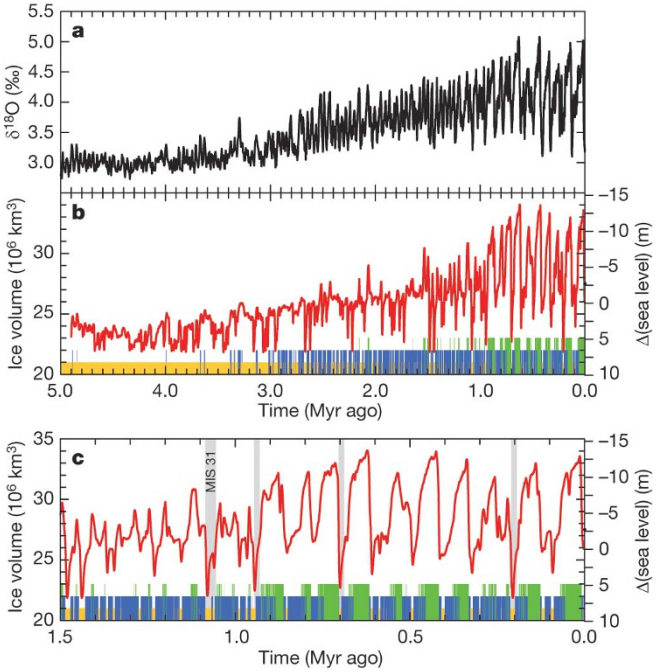

Figure 2 | Simulated total Antarctic ice volume over the past five million years. a, Stacked deep-sea-core benthic δ^{18}O (ref. 18). **b**, Total Antarctic ice volume (red line) in a long-term simulation with variations of sub-ice melt and other forcings parameterized mainly from the deep-sea-core δ^{18}O record. Equivalent changes in global sea level are shown on the right, accounting for the fraction of grounded ice above sea level compared to that below sea level[1]. Bars along the x-axis indicate conditions at a single location (78.0° S, 169.4° E), shifted one grid box to the east of AND-1B[11] to avoid poorly resolved Ross Island shorelines (yellow, open ocean; blue, floating ice shelf; green, grounded ice). Yellow and blue/green here correspond to the AND-1B diatomite (yellow) and diamictite (green) intervals in Fig. 2 of ref. 11. **c**, As **b** but with the time axis expanded over the past 1.5 Myr. Grey shading indicates simulated super-interglacials, beginning with MIS 31[21].

parameterizations using δ^{18}O and austral insolation as inputs (equations (1) and (2) in Methods).

Factors controlling past variations of oceanic sub-ice melt on ~10^4 yr timescales are less certain. Sub-ice oceanic melting is affected in part by circum-Antarctic deep-water (CDW) warmth and its incursions onto continental shelves[19]. We argue that CDW and sub-ice melt have been mainly controlled by far-field climatic influences that vary in step with Northern Hemispheric glacial–interglacial cycles (see Methods). Without identifying the explicit link (which may involve atmospheric CO_2, meridional overturning circulation, sea level, or other global-scale teleconnections), we hypothesize that temporal variations of Antarctic sub-ice ocean melt rates are represented by records that correlate with Northern Hemispheric glacial variations, that is, deep-sea-core δ^{18}O (equations (6)–(8) in Methods). A minor additional influence on sub-ice melt from austral summer orbital insolation anomalies[20] is also needed to produce precessional cyclicity like that observed during marine isotope stage 31 (MIS 31) around 1 Myr ago[11,21]. Our forcing is warmest during the early Pliocene warm period (~5 to ~3 Myr ago) due to light δ^{18}O values at that time; however, the parameterizations are based more on Pleistocene variations, and may not fully represent the warm Pliocene if unique processes (for example, persistent El Niño)[9] were involved.

With long-term forcing variations mainly following deep-sea-core δ^{18}O (ref. 18), the ice-sheet model is continuously integrated over the past 5 Myr (Fig. 2). Except for small variations along the Wilkes margin[22] and in inlets such as Prydz bay[23], East Antarctica is stable throughout the simulation and nearly all of the ice-volume variability is due to West Antarctica. Several key aspects of the model time series agree with the AND-1B core[11]. There is an overall progression from predominantly smaller WAIS sizes to larger. Furthermore, intervals of WAIS collapse with little or no marine ice are much more common from ~5 to 3 Myr ago, which is consistent with intervals in the drillcore dominated by diatomaceous sediments indicating warmer sea surface temperatures, little or no summer sea ice, and an open marine Ross embayment[11]. In fact, the two thickest diatomaceous intervals in the core, between ~4.3 and 3.4 Myr ago, correspond to the period with the most frequent and prolonged WAIS collapses simulated by the model. These collapses could well be continuous if additional Pliocene warm-period forcing was added[9]. After 3 Myr ago, there are longer intervals with modern-to-glacial ice volumes, that is, with ice-shelf or grounded-ice cover at or near the AND-1B site (Fig. 2), again in rough agreement with the increasing predominance of diamictite after 3 Myr ago indicating overriding ice or a proximal grounding zone[11].

Brief WAIS super-interglacial collapses occur after 3 Myr ago but with decreased frequency. In some cases, these precisely match the thinner diatomaceous intervals in the AND-1B core, including the well-dated MIS 31 event at 1.07 Myr ago[11,21]. The large 100-kyr fluctuations of the past million years are similar to those modelled in earlier studies[6,7,17]. The last retreat of WAIS from ~15 kyr ago to the present roughly matches the observed retreat of Ross Sea grounding lines[24,25], and is particularly realistic with modifications described in Supplementary Information section 6.

The model predicts several major WAIS collapses during Pleistocene interglacials (Fig. 2c), at times when δ^{18}O minima coincide with strong

austral summer insolation anomalies. The simulated collapse at MIS 31 corresponds well with core evidence[11,21], both in terms of timing and magnitude, but more recent collapses (for example, ~200 kyr ago) do not always coincide with the late-Pleistocene interglacials (~125 kyr ago and ~400 kyr ago) usually suspected of harbouring such events[10,26,27]. Thus, while the total number of collapses is reasonable, their sometimes imprecise timings may reflect the limitations of our simple forcing parameterizations, including uncertainties in the 40-kyr phase relationship of Antarctic sub-ice melt to deep-sea-core $\delta^{18}O$ records, and the influence of local orbital insolation forcing. Although the model clearly captures the overall ~40-kyr periodicity seen in the AND-1B record, the precise phasing between Antarctic ice sheet variations and Northern Hemispheric climate changes remains uncertain. In some instances, the timing of our simulated super-interglacials may be an artefact of the phasing between the imposed $\delta^{18}O$ and austral summer insolation forcings. Recent observational and modelling studies on the relative timing of Northern Hemisphere ice volume variations, ocean meridional overturning and orbital forcing[28–30] are pertinent to this issue, but with no clear consensus to date. These relationships could also be explored in future work with global climate models in combination with regional circum-Antarctic and sub-ice-shelf ocean modelling[14,19], to better ascertain the effects of Northern Hemispheric glacial cycles, orbital forcing and greenhouse gas concentrations on regional Antarctic conditions.

To better focus on the Ross embayment and the AND-1B site[11], we ran higher-resolution (10 km) nested ice sheet-shelf simulations for particular times, with boundary conditions at the domain edges obtained from the long-term all-Antarctic simulation. Figure 3 illustrates a wide range of WAIS states, from weak glacial, full WAIS collapse, to modern conditions. The modern network and behaviour of Siple Coast ice streams and Transantarctic outlet glaciers is well resolved (Fig. 3f), with some ice streams stagnating and re-activating over the several thousand years of the nested run[31] (Supplementary Videos 3 and 4). Ross ice shelf velocities are also similar to observations, as is the central streamline dividing Siple (West Antarctic) and Transantarcic (East Antarctic) ice[31]. The finer ice grid resolves the general ice flow around Ross Island, although the details of flow are not fully resolved within the narrow confines of McMurdo Sound containing AND-1B and other drill sites[11,21]. When shelf ice is present at AND-1B (Fig. 3i), offshore flow just to the east is always northward, with ice originating from major Transantarctic outlet glaciers to the south (Byrd, Skelton, Mulock). This offshore flow pattern and its Transantarctic provenance prevail whenever there is shelf ice around Ross Island.

The dominant regional control is the overall strength of sub-ice oceanic melting in the Ross embayment, which causes both Siple- and Transantarctic-sourced ice to recede or advance in concert over the eastern and western sides of the embayment, respectively. It is very rare for one type or the other to dominate. Thus, although the provenance of shelf ice around Ross Island may be insensitive to the overall WAIS state, the basic presence or absence of shelf ice at the AND-1B site[11] is a good qualitative indicator of maxima and minima in WAIS ice volume (Fig. 2). Other sites not yet cored in the central Ross embayment may offer even better potential for uniquely identifying times of WAIS collapse (Supplementary Fig. 3). These simulations show how

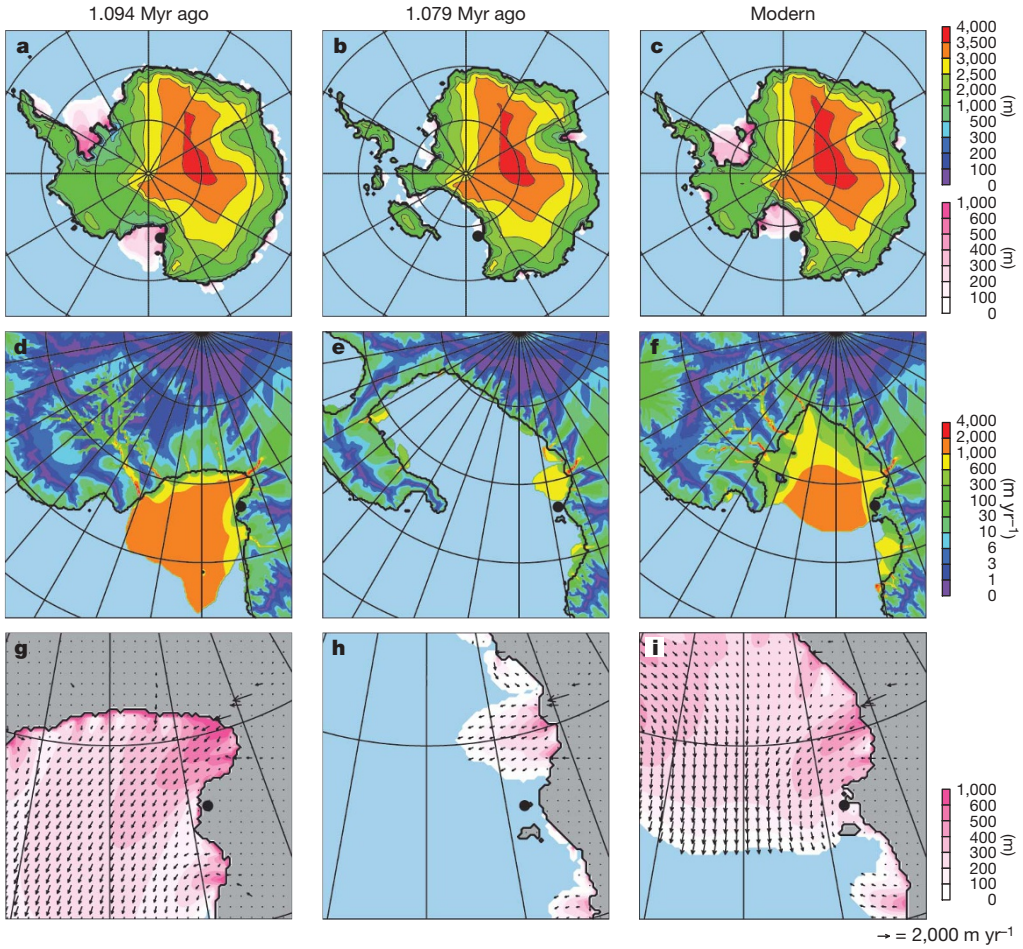

Figure 3 | Snapshots at particular times from the long-term simulation in Fig. 2. Shown are 1.094 Myr ago, 1.079 Myr ago (MIS 31 retreat) and modern. **a–c**, Grounded ice elevations and floating ice thicknesses, shown respectively (in m) by upper and lower colour scale on right. **d–f**, Surface ice speeds (m yr^{-1}), from higher-resolution (10 km) nested runs over the Ross embayment for the same three times, showing the whole nested domain. **g–i**, Floating ice thicknesses (m) and velocity vectors from the nested simulations, enlarged over the western Ross embayment. Vectors are shown only every third grid point for clarity. The location of AND-1B is shown by the black dot.

local observables in the AND-1B and other cores relate to overall WAIS evolution. In particular, our results imply that the presence or absence of grounded or floating ice in the vicinity of McMurdo Sound is indeed linked to WAIS ice volume, and that open-water conditions in the Ross Sea are indicative of partial to complete collapse of the WAIS.

Some of our results are independent of the parameterized temporal variations in long-term forcing. For example, the estimated magnitudes of sub-ice oceanic melt rates needed to produce full WAIS amplitudes (Fig. 1 and Methods) form a point of reference for future modelling. Another independent result is the tendency for the WAIS to experience relatively rapid transitions within one to a few thousand years, as forcing is smoothly varied. This includes transitions into and out of collapsed states, and from full glacial to modern-like ice extents. A collapse from modern conditions occurs when sub-ice ocean melting increases from 0.1 to 2 m yr^{-1} under shelf interiors, and from 5 to 10 m yr^{-1} near exposed shelf edges (M_p and M_e respectively, in equations (3), (7) and (8) in Methods). Recent melt rates under small Antarctic ice shelves are inferred to be increasing dramatically[15,16]. The relationship between sub-ice melt rates and ocean temperatures is just beginning to be explored[19], but those data[15,16] and simplified modelling[14] suggest relationships on the order of 10 m yr^{-1} °C^{-1} for smaller shelves, and 0.4 m yr^{-1} °C^{-1} for whole-shelf averages under the major Ross and Filchner-Ronne shelves. Dividing our interior-melt (M_p) increase of 1.9 m yr^{-1} by the latter sensitivity of 0.4 m yr^{-1} °C^{-1} suggests that the WAIS will begin to collapse when nearby ocean temperatures warm by roughly 5 °C. Global climate and regional ocean modelling is needed to predict when and if future ocean temperatures and melt rates under the major Antarctic ice shelves will increase by these amounts, and if so, for how long.

METHODS SUMMARY

The scaled dynamical equations for sheet flow (shallow ice approximation) and shelf flow can be combined heuristically[12]. However, for efficiency in these long-term simulations, they are applied separately depending on whether ice is grounded or floating. Despite this simplification and coarse grids, the effects of the grounding-line boundary layer are captured by imposing a mass-flux condition across the grounding line following ref. 5, which sets ice velocities there as a function of ice thickness. To include important effects of ice-shelf buttressing, the imposed grounding-line velocities are reduced depending on the ratio of longitudinal stress to its free-floating value[5] (see Supplementary Information). The model also contains three other standard components: (1) an ice-mass advection equation predicting ice thickness and accounting for surface accumulation minus ablation and basal melt, (2) an ice temperature equation including horizontal advection, vertical diffusion and shear heating, and (3) a bedrock elevation equation with local relaxation towards isostatic equilibrium and elastic lithospheric flexure[6,7]. There is no explicit basal hydrology, other than allowing basal sliding only where the bed is at the melt point.

Equilibrium ice-free topography and bathymetry are prescribed from the modern BEDMAP database[1], by removing all ice and allowing the bed to rebound isostatically. Prescribed basal sliding coefficients crudely represent the likely spatial distribution of deformable sediment versus hard bedrock, that is, sediment where the ice-free rebounded topography is below sea level (mostly WAIS) and bedrock where above (mostly East Antarctic ice sheet). In addition, intermediate basal stiffness is prescribed in the Pine Island/Thwaites drainage sector and Transantarctic inlets below sea level, to improve modern grounding-line locations and glacier velocities there. Past surface mass balance and sub-ice-shelf oceanic melting are parameterized using deep-sea-core $\delta^{18}O$ and orbital insolation variations (see Methods). The model is run on a polar stereographic grid, with 40 km resolution for continental and 10 km for nested experiments.

Full Methods and any associated references are available in the online version of the paper at www.nature.com/nature.

Received 12 August 2008; accepted 8 January 2009.

1. Lythe, M. B. *et al.* BEDMAP: A new ice thickness and subglacial topographic model of Antarctica. *J. Geophys. Res. Solid Earth* 106 (B6) 11335–11351 (2001).
2. Mercer, J. H. West Antarctic ice sheet and CO_2 greenhouse effect: A threat of disaster. *Nature* **271,** 321–325 (1978).
3. Weertman, J. Stability of the junction of an ice sheet and an ice shelf. *J. Glaciol.* **13,** 3–11 (1974).
4. Oppenheimer, M. & Alley, R. B. The West Antarctic ice sheet and long term climate policy – An editorial comment. *Clim. Change* **64,** 1–10 (2004).
5. Schoof, C. Ice sheet grounding line dynamics: Steady states, stability, and hysteresis. *J. Geophys. Res.* **112,** F03S28, doi:10.1029/2006JF000664 (2007).
6. Ritz, C., Rommelaere, V. & Dumas, C. Modeling the evolution of Antarctic ice sheet over the last 420,000 years: Implications for altitude changes in the Vostok region. *J. Geophys. Res.* 106 (D23) 31943–31964 (2001).
7. Huybrechts, P. Sea-level changes at the LGM from ice-dynamic reconstructions of the Greenland and Antarctic ice sheets during the glacial cycles. *Quat. Sci. Rev.* **21,** 203–231 (2002).
8. Anderson, J. B. *Antarctic Marine Geology* (Cambridge Univ. Press, 1999).
9. Ravelo, A. C. *et al.* Regional climate shifts caused by gradual global cooling in the Pliocene epoch. *Nature* **429,** 263–267 (2004).
10. Scherer, R. P. Quaternary and Tertiary microfossils from beneath Ice Stream-B – Evidence for a dynamic West Antarctic Ice-Sheet History. *Glob. Planet. Change* **90,** 395–412 (1991).
11. Naish, T. *et al.* Obliquity-paced, Pliocene West Antarctic ice sheet oscillations. *Nature* (this issue).
12. Pollard, D. & DeConto, R. M. in *Glacial Sedimentary Processes and Products* (eds Hambrey, M., Christoffersen, P., Glasser, N. & Hubbard, B.) 37–52 (Spec. Publ. 39, International Association of Sedimentologists, Blackwell Publishing, 2007).
13. Pattyn, F. A new three-dimensional higher-order thermomechanical ice sheet model: Basic sensitivity, ice stream development, and ice flow across subglacial lakes. *J. Geophys. Res.* **108** (B8), 2382, doi:10.1029/2002JB002329 (2003).
14. Beckmann, A. & Goose, H. A parameterization of ice shelf-ocean interaction for climate models. *Ocean Model.* **5,** 157–170 (2003).
15. Rignot, E. & Jacobs, S. S. Rapid bottom melting widespread near Antarctic ice sheet grounding lines. *Science* **296,** 2020–2023 (2002).
16. Shepherd, A., Wingham, D. & Rignot, E. Warm ocean is eroding West Antarctic Ice Sheet. *Geophys. Res. Lett.* **31,** L23402, doi:10.1029/2004GL021106 (2004).
17. Philippon, G. *et al.* Evolution of the Antarctic ice sheet throughout the last deglaciation: A study with a new coupled climate - north and south hemisphere ice sheet model. *Earth Planet. Sci. Lett.* **248,** 750–758 (2006).
18. Lisiecki, L. E. & Raymo, M. E. A. Pliocene-Pleistocene stack of 57 globally distributed benthic $\delta^{18}O$ records. *Paleoceanography* **20,** PA1003, doi:10.1029/2005PA001153 (2005).
19. Holland, P. R. & Jenkins, A. The response of ice shelf basal melting to variations in ocean temperature. *J. Clim.* **21,** 2558–2572 (2008).
20. Laskar, J. *et al.* A long-term numerical solution for the insolation quantities of the Earth. *Astron. Astrophys.* **428,** 261–285 (2004).
21. Scherer, R. P. *et al.* Antarctic records of precession-paced insolation-driven warming during early Pleistocene Marine Isotope Stage 31. *Geophys. Res. Lett.* **35,** L03505, doi:10.1029/2007GL032254 (2008).
22. Hill, D. J., Haywood, A. M., Hindmarsh, R. C. A. & Valdes, P. J. in *Deep Time Perspectives on Climate Change: Marrying the Signals from Computer Models and Biological Proxies* (eds Williams, M., Haywood, A. M., Gregory, F. J. & Schmidt, D. N.) 517–538 (Micropaleontological Society Special Publications, Geological Society, 2007).
23. O'Brien, P. E. *et al.* Late Neogene ice drainage changes in Prydz Bay, East Antarctica and the interaction of Antarctic ice sheet evolution and climate. *Palaeogeogr. Palaeoclimatol. Palaeoecol.* **245,** 390–410 (2007).
24. Conway, H. *et al.* Past and future grounding-line retreat of the West Antarctic Ice Sheet. *Science* **286,** 280–283 (1999).
25. McKay, R. M. *et al.* Retreat history of the Ross Ice Sheet (Shelf) since the Last Glacial Maximum from deep-basin sediment cores around Ross Island. *Palaeogeogr. Palaeoclimatol. Palaeoecol.* **260,** 245–261 (2008).
26. Hearty, P. J. *et al.* Global sea-level fluctuations during the Last Interglaciation (MIS 5e). *Quat. Sci. Rev.* **26,** 2090–2112 (2007).
27. Raynaud, D. *et al.* in *Earth's Climate and Orbital Eccentricity: The Marine Isotope Stage 11 Question* (eds Droxler, A. W., Poore, R. Z. & Burckle, L. H.) 27–40 (American Geophysical Union, 2003).
28. Lisiecki, L. E., Raymo, M. E. & Curry, W. B. Atlantic overturning responses to Late Pleistocene climate forcings. *Nature* **456,** 85–88 (2008).
29. Huybers, P. & Denton, G. Antarctic temperature at orbital timescales controlled by local summer duration. *Nature Geosci.* **1,** 787–792 (2008).
30. Kawamura, K. *et al.* Northern Hemisphere forcing of climatic cycles in Antarctica over the past 360,000 years. *Nature* **448,** 912–916 (2007).
31. Hulbe, C. & Fahnestock, M. Century-scale discharge stagnation and reactivation of the Ross ice streams, West Antarctica. *J. Geophys. Res.* **112,** F03S27, doi:10.1029/2006JF000603 (2007).
32. Pollard, D. & DeConto, R. M. Hysteresis in Cenozoic Antarctic ice sheet variations. *Glob. Planet. Change* **45,** 9–21 (2005).

Supplementary Information is linked to the online version of the paper at www.nature.com/nature.

Acknowledgements We thank T. Naish and R. Powell for discussions on this work, and P. Barrett for comments on the manuscript. This work was funded by the US National Science Foundation under awards ATM-0513402/0513421, ANT-034248 and ANT-0424589.

Author Information Reprints and permissions information is available at www.nature.com/reprints. Correspondence and requests for materials should be addressed to D.P. (pollard@essc.psu.edu).

METHODS

Modern climatic forcing: temperature and precipitation. Modern forcing fields of annual surface mass-balance and temperature are specified using simple empirical parameterizations, and then varied in the past depending on ice-core or deep-sea-core time series, similarly to previous studies[6,7]. Annual surface temperatures (°C) are[33]

$$T = T_m + 34.46 - 0.00914\, h_s - 0.68775\,|\phi| + 0.1\,\Delta q_a + 10\Delta s/125 \quad (1)$$

where $T_m = 0$ °C, h_s is elevation (m), $|\phi|$ is latitude (°S), Δq_a is annual orbital insolation anomaly from present at 80° S (W m^{-2}), and Δs is sea-level departure from present (m) representing atmospheric CO_2 (see equation (6) below). Annual precipitation P (m yr^{-1}) is parameterized via temperature[34]:

$$P = 1.5 \times 2^{(T - T_m)/10} \quad (2)$$

The fraction of precipitation falling as snow, and annual surface melt if any, are computed from T using a positive-degree-day (PDD)[35] method with coefficient 0.005 m per degree-day. A sinusoidal seasonal temperature cycle of amplitude $0.1\Delta q_s$ (°C) is assumed, where Δq_s is January-minus-July 80° S insolation (W m^{-2}). (Very little surface-melt occurs in our simulations, because summer air temperatures remain below freezing everywhere.)

Modern climatic forcing: sub-ice-shelf oceanic melt. A new parameterization of oceanic melt rates is used, based on the degree of protection by islands and bays, and distance to ice-shelf edge[17]. Although simple, it captures basic features of other studies, such as rapid melting near edges[14,19,36,37], and yields reasonable modern shelf distributions. Modern sub-ice melt M (m yr^{-1}) is

$$M = (1 - z_d)\left[(1 - z_e)\, M_p + z_e\, M_e\right] + z_d\, M_d \quad (3)$$

where the 'deep-ocean' weighting is

$$z_d = \max[\,0,\ \min[\,1,\ (h_b - 1400)/200\,]\,] \quad (4)$$

and the 'exposed-shelf' weighting is

$$z_e = \max[\,0,\ \min[\,1,\ (A - 80)/30\,]\,]\ e^{-D/100} \quad (5)$$

Here max[x, y] indicates the greater of x and y, and min[x, y] indicates the lesser. The 3 modern oceanic melt rates M_p, M_e and M_d in equation (3) are for protected, exposed-shelf and deep-ocean areas, respectively, given by $M_p = 0.1$ m yr^{-1}, $M_e = 5$ m yr^{-1}, and $M_d = 5$ m yr^{-1}. In equations (4) and (5), h_b is bathymetry (m), A is the angle (degrees) subtended by the set of all straight lines from the point in question that reach open ocean without encountering land or grounded ice, and D (km) is the sub-ice distance to the closest open-ocean point. The angle A is the main way we achieve realistic modern ice-shelf edges. Around most major Antarctic shelf-edges today, A is ~90° to 100°; whether this coincidence has a physical basis requires exploration with regional ocean models.

Past climatic forcing: sea level, temperature and precipitation. We need to prescribe long-term variations of sub-ice oceanic melt rates, sea level, air temperature and precipitation over the past 5 Myr. On longer timescales, atmospheric CO_2 levels outside the Plio-Pleistocene range (~180–380 p.p.m.v.), basal sediment changes, and tectonic uplift or subsidence are probably important, but were probably minor through the Plio-Pleistocene. As mentioned above, our Pleistocene-centric parameterizations may underestimate warmth during the early Pliocene ~5–3 Myr ago when CO_2 levels rose to ~380 p.p.m.v. (ref. 9).

Sea-level variations have been dominated by Northern Hemispheric ice volume, and are assumed proportional to deep-sea core $\delta^{18}O$ and calibrated as in equation (6). Past variations of Antarctic annual surface temperatures are included in equation (1), proportional to a combination of atmospheric CO_2 (which is represented by $\delta^{18}O$ via sea level in equation (1), since all three are highly correlated in the Pleistocene at least) and the annual 80° S insolation anomaly. Past variations in precipitation depend on air temperature, just as for modern spatial variations (equation (2)).

Past climatic forcing: sub-ice-shelf oceanic melt. The long-term controls of sub-ice-shelf melting are just beginning to be explored[14,19,37]. Here we propose a parameterization based on simple reasoning and sensitivity tests of WAIS retreat since 15 kyr ago. This last deglacial retreat is the only well-documented WAIS variation on 10^4-year time scales. It cannot have been driven by surface mass balance, because Antarctic precipitation has increased, not decreased, and there has been negligible surface melt during this time. Model sensitivity tests show that sea-level rise alone, and/or the influence of warming temperatures on ice viscosity and basal sliding, account for only a small fraction of the observed retreat. Therefore, increases in sub-ice melting must have been key. They could reasonably have been driven either by regional Southern Hemispheric orbital insolation changes, or by global-scale far-field influences. Southern Hemispheric insolation is unlikely to have been the dominant driver, because (1) the summertime 80° S anomaly from present was small and negative between 15 and 2 kyr ago, and (2) the annual 80° S anomaly, with minimum at 28.7 kyr ago and maximum at 9.5 kyr ago (ref. 20), would have caused retreat to commence too early (before ~19 kyr ago) judging from Ross Sea grounding-line history (~10 kyr ago)[24,25]. This is borne out by sensitivity tests (Supplementary Fig. 5) in which austral insolation is used as the sole driver of sub-ice melt, and results over the past 15,000 years are unreasonable. Realistic retreat is obtained only if sub-ice melt varies in step with far-field forcing.

This suggests that sub-ice melt has been controlled not by local forcing or austral insolation, but by far-field climatic influences that vary in step with Northern Hemispheric glacial–interglacial cycles at least since ~2.5 Myr ago. The latter is represented here by a stacked deep-sea-core $\delta^{18}O$ record spanning the past 5 Myr (ref. 18). A small influence of austral summer insolation[20] is added to produce minor observed 20-kyr cyclicity during warm events such as MIS 31[21]. First, a weighting index w_g is defined by

$$w_g = \max\left[\,0,\ \min\left[\,2,\ 1 + \Delta s/85 + \max\left(0,\ \Delta q_j/40\right)\,\right]\,\right] \quad (6)$$

where $\delta^{18}O$ is represented by Δs, the sea-level departure from present (m, scaled to $\delta^{18}O$ with last-glacial-maximum 125 m lower than present), and Δq_j is the January 80° S insolation anomaly from present (W m^{-2}). Sub-ice-melt rates for protected, exposed-shelf and deep-sea areas ($[M_p, M_e, M_d]$ respectively, in m yr^{-1}) are specified as [0,0,2] for maximum-glacial conditions, [0.1,5,5] for modern, and [2,10,10] for extreme-interglacial conditions. Then the triplet used in equation (3) to determine M for any past time is

$$\left[M_p, M_e, M_d\right] = (1 - w_g)\,[0,\ 0,\ 2] + w_g\,[0.1,\ 5,\ 5] \quad \text{if } 0 \le w_g < 1 \quad (7)$$

or

$$\left[M_p, M_e, M_d\right] = (2 - w_g)\,[0.1,\ 5,\ 5] + (w_g - 1)\,[2,\ 10,\ 10] \quad \text{if } 1 \le w_g \le 2 \quad (8)$$

The modern triplet values are chosen to yield reasonable results for today's Ross and Filchner-Ronne ice shelves. The glacial and warm triplets and the form of w_g in equation (6) are chosen so that the model just attains full-glacial WAIS extents and complete interglacial collapses in long-term simulations and in Fig. 1. These values cannot be changed by large amounts without substantial degradation of our results.

33. Huybrechts, P. Glaciological modelling of the late Cenozoic East Antarctic Ice Sheet: Stability or dynamism? *Geogr. Ann. A* **75,** 221–238 (1993).
34. Huybrechts, P. *Report of the Third EISMINT Workshop on Model Intercomparison* (European Science Foundation, 1998).
35. Marshall, S. J. & Clarke, G. K. C. Ice sheet inception: Subgrid hypsometric parameterization of mass balance in an ice sheet model. *Clim. Dyn.* **15,** 533–550 (1999).
36. Macayeal, D. R. & Thomas, R. H. The effects of basal melting on the present flow of the Ross Ice Shelf, Antarctica. *J. Glaciol.* **32,** 72–86 (1986).
37. Dinniman, M. S., Klinck, J. M. & Smith, W. O. Influence of sea ice cover and icebergs on circulation and water mass formation in a numerical circulation model of the Ross Sea, Antarctica. *J. Geophys. Res.* **112,** C11013, doi:10.1029/2006JC004036 (2007).